

Hot spots revealed by simultaneous experimental measurement of the two-dimensional concentration and temperature fields of an exothermic chemical front during finger-pattern formation

P. Grosfiils,^{1,*} F. Dubois,¹ C. Yourassowsky,¹ and A. De Wit^{2,†}

¹*Microgravity Research Center, Chimie Physique E.P. CP 165/62, Université Libre de Bruxelles (ULB), Avenue F.D. Roosevelt 50, 1050 Brussels, Belgium*

²*Nonlinear Physical Chemistry Unit, Service de chimie physique et biologie théorique, Faculté des Sciences, Université Libre de Bruxelles (ULB), CP 231, 1050 Brussels, Belgium*

(Received 17 June 2008; published 16 January 2009)

A noninvasive optical technique combining digital interferometry in transmission and transparency measurement of concentration is developed to analyze spatiotemporal dynamics of physicochemical systems. This technique allows one to measure simultaneously the two-dimensional (2D) dynamics of concentration and temperature fields in both reactive and nonreactive systems contained inside a transparent cell. When used to experimentally analyze buoyancy-driven fingering of an exothermic autocatalytic chemical front, this method reveals in the 2D temperature field the presence of hot spots where the temperature locally exceeds the adiabatic one.

DOI: [10.1103/PhysRevE.79.017301](https://doi.org/10.1103/PhysRevE.79.017301)

PACS number(s): 47.20.Bp, 47.70.Fw, 82.40.-g, 42.40.Kw

Convective flows due to Rayleigh-Taylor, Rayleigh-Bénard, or double-diffusive types of hydrodynamic instabilities can be triggered in nonreactive solutions by spatial gradients of concentration and temperature. Such phenomena are genuinely observed in numerous applications ranging from engineering systems to Earth mantle convection and atmospheric or ocean convective motions, to name a few [1,2]. In reactive systems, chemically driven gradients of concentration and temperature can also trigger hydrodynamic flows that in turn affect the spatiotemporal dynamics of the system as observed in electrochemical systems [3], simple $A+B \rightarrow C$ fronts [4–6], combustion or polymerization fronts [7–10], or autocatalytic redox reaction fronts [10–21]. Indeed, the composition and temperature variations in the course of an exothermic reaction are responsible for changes in the density which, in the gravity field, can give rise to buoyancy induced flows. Recent work have shown that new nontrivial spatiotemporal dynamics can result from the competition between solutal and thermal buoyancy-driven convective effects in such reactive systems [17–25].

Clear experimental demonstration of the role of heat effects in such dynamics is, however, impaired by the difficulty in measuring simultaneously experimentally the full spatial evolution of concentration and temperature fields. While access to the dynamics of concentration fields is readily obtained by means of a dye or of a specific color indicator, for instance, temperature measurements in fluid flows is usually accomplished by means of thermocouples that are immersed in the fluid. However, the use of thermocouples suffers from the drawbacks that the direct contact with the fluid can alter the flow, and that temperature field can only be measured at a local fixed position. To yield insight into the global two-dimensional (2D) spatial evolution of temperature fields, some authors have previously used infrared imaging [14,16] or thermocolor materials [13] to track temperature changes

around exothermic chemical fronts. The first technique has, however, the drawback to get information only at the surface layer of the solution while the second method is intrusive. It needs to add thermo-sensitive species to the solution or insert a capillary containing these species in the reactor but then the information on temperature is obtained only in one direction. Information on temperature fields around autocatalytic fronts have also been obtained through magnetic resonance imaging [26,27]. In this latter case, however, the resolution needed temperature variations larger than 1 K. In addition, in all abovementioned experiments, the technique used allowed us to measure either the concentration field or the temperature field but not both of them simultaneously.

Here we present a nonintrusive optical technique that allows one to obtain simultaneous insight into the 2D spatiotemporal evolution of both the concentration and temperature fields in a liquid system contained in a transparent setup. We next show how this technique has allowed us to uncover the presence of hot spots (i.e., localized zones where the temperature is locally larger than the adiabatic one) in buoyancy-driven fingering of an autocatalytic chemical front.

Our optical technique is based on the combination of interferometry in transmission and of a transparency measurement. The interferometry analysis provides the refractive index change that is due to the combination of temperature and composition changes. The transmittivity measurement allows one to quantify the composition in such a way that the appropriate combination of the measures results in the knowledge of the temperature field. Our technique is applied here to obtain in detail the temporal evolution of both the 2D concentration and temperature fields across an autocatalytic chemical front of the chlorite-tetrathionate (CT) reaction, an exothermic redox reaction known to exhibit fingering phenomena [17–19,21,22,25]. Information on the full 2D evolution of the temperature allows one to obtain insight into the fingering dynamics and show that hot spots are present at the cusp of the fingered front, a phenomenon which remains here unnoticed by a thermocouple measurement of the local temperature at one point.

*pgrosfi@ulb.ac.be

†adewit@ulb.ac.be

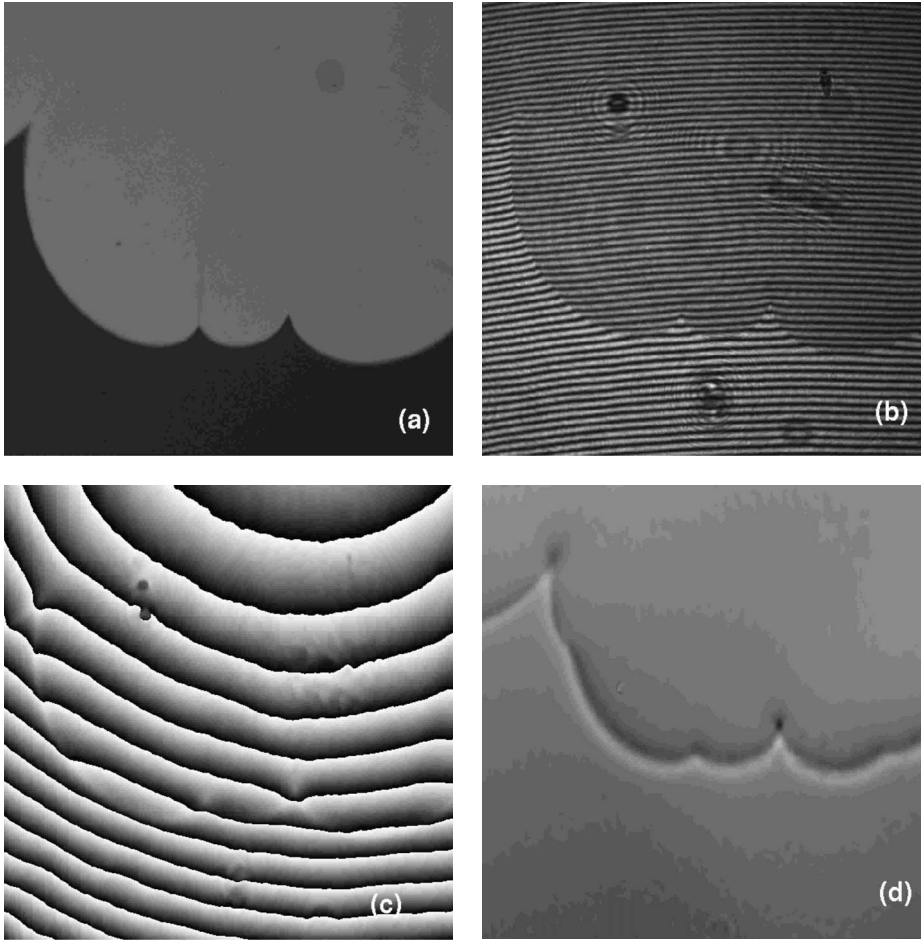


FIG. 1. Fingering of a chemical front visualized as an absorption image (a), an interferometric image (b), an optical phase image (c), and a corrected optical phase image (d).

The experimental cell consists of a Hele-Shaw cell made of two transparent glass plates separated by a gap of 1 mm and oriented vertically in the gravity field. The cell is filled with the reactants of the CT reaction following a recipe previously used for studies of fingering [17]. A descending front is initiated by an electric current passing through two parallel electrodes fixed at the upper edge of the cell. This generates a downward moving planar front that quickly becomes buoyantly because of an unstable stratification of heavier products on top of lighter reactants. The front deforms then into a cellular structure (see Fig. 1) induced by convective motions of the fluid. The CT system is known to belong to the family of antagonist reactions for which solutal and thermal contributions to the density jump across the front have opposite signs [11,25].

To have insight into the dynamics of such exothermic fronts, we use digital interferometry which allows visualization and measurement of the phase difference $\Delta\phi$ between two beams, one passing through the sample of depth L along z with refractive index $n(x,y,z)$ and the other one passing in the air

$$\begin{aligned}\Delta\phi(x,y) &= \frac{2\pi}{\lambda} \int_0^L [n(x,y,z) - n_0] dz, \\ &= \frac{2\pi L}{\lambda} \Delta\bar{n}(x,y),\end{aligned}\quad (1)$$

where n_0 is the refractive index of the air, λ the wavelength

of the light, and $\bar{n}(x,y)$ is the refractive index averaged over the depth of the sample.

When variations of the refractive index are caused by variations of a scalar field f (similar to the temperature or concentration), this latter can be obtained from Eq. (1) as

$$\Delta f(x,y) = \frac{\lambda}{2\pi L} \left(\frac{\partial \bar{n}}{\partial f} \right)^{-1} \Delta\phi(x,y). \quad (2)$$

In most applications, the refractive index is assumed to depend only on one single field such as the concentration c or temperature T typically. This assumption allows us to identify interference fringes with lines of constant T or constant c , for instance [28]. However, such an assumption should, in principle, not be valid in the situation where density gradients are due to combined solutal and thermal effects as in the case of exothermic reaction fronts. A way to solve the problem is to take advantage of the dependence in frequency of the refractive index. Some elaborate interferometric techniques that take into account the refractive index-frequency relation [29] use two relations obtained by expressing the equation

$$\Delta\phi(\lambda_i) = \frac{2\pi L}{\lambda_i} \left(\frac{\partial n(\lambda_i)}{\partial c} \Delta c + \frac{\partial n(\lambda_i)}{\partial T} \Delta T \right) \quad (3)$$

for two different wavelengths λ_1 and λ_2 . These two equalities are then combined to resolve simultaneously both the temperature and the concentration fields. However, these

techniques require more complicated optical systems. In addition there is no possible control of the frequency dependence of the refractive index. It results that the accuracy on the final result can be low.

In this Brief Report both the concentration and the temperature fields are measured by a technique during fingering of an exothermic reaction front. The measurement of the two scalar fields is still based on Eq. (3) but taken now at one fixed wavelength while $\Delta\phi$ and Δc are determined by different optical apparatus in a simple optical arrangement. Explicitly, the system combines a Mach-Zehnder interferometer ($\lambda=633$ nm) with a transference imaging with a blue light-emitting diode (LED). The optical system is combined with a CCD camera for image capture.

The two optical apparatus rely upon the variation of certain properties of the fluid along the path traveled by the ray of light. Transmission gives a spatial distribution of absorption of the light by the fluid. The image is obtained by illuminating the Hele-Shaw cell with a blue LED (470 nm) and recording the intensity of the light transmitted through the liquid. The blue light has been chosen so as to maximize the contrast between the reactants colored in red and the products, which are blue. Absorption is assumed to be independent of temperature and to depend only on the change in the product concentration Δc . Interferometry is used to obtain $\Delta\phi$, and the temperature field can then be reconstructed via the relationship

$$\frac{2\pi L}{\lambda} \left(\frac{\partial n}{\partial T} \right) \Delta T = \Delta\phi - \frac{2\pi L}{\lambda} \left(\frac{\partial n}{\partial c} \right) \Delta c. \quad (4)$$

Figure 1(a) shows an image of the fingers obtained by absorption. In this image the front propagates downwards and the products appear bright. On the corresponding interferometric image (b), the interferometer is aligned in such a way that it provides initially a dense horizontal fringe pattern. Then the relevant optical phase shift $\Delta\phi$ is obtained by the Fourier method (c) [30,31]. The phase image is corrected by a reference image in order to eliminate the possible misalignment of the Hele-Shaw cell window. The final result (d) is an image of the corrected phase the intensity of which is proportional to the variation of the refractive index. Thanks to the absorption image, the position of the reaction front and of the corresponding concentration field are extracted. This information is next used to eliminate the contribution of solutal effects to the phase shift and isolate the 2D temperature field.

For a quantitative measurement of the temperature and of density a knowledge of the variation of the index of refraction with these quantities is required. We have measured the values of the refractive index of the fluid before and after reaction using an Abbe refractometer. The results show that the refractive index varies slightly with the concentration, and the value measured is very close to the value for water (with a precision 10^{-4}). Therefore, under the assumption of diluted solutions one can assume a linear variation of the refractive index with concentration $\partial n / \partial c \approx \text{const.}$ and with temperature $\partial n / \partial T \approx \text{const.}$ Consequently, Eq. (4) reduces to $a_1 \Delta T = \Delta\phi - a_2 \Delta c$, where a_1 and a_2 are constants. Although these constants could, in principle, be computed from the

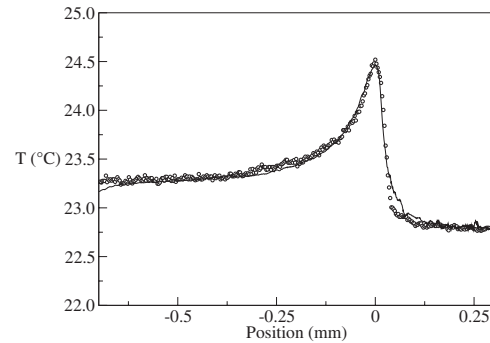


FIG. 2. The temperature across an exothermic front traveling from left to right measured by interferometry (dots) and via a thermocouple (line). The thermocouple measurement is used to calibrate the interferometric measures.

underlying parameters, a more accurate evaluation is obtained by performing an independent measure of T across the chemical front by a thermocouple (Fig. 2). This measure determines the temperature along a line across the front with a precision of ± 0.05 °C. To calibrate the temperature field obtained by interferometry, the values of the temperature away from the front (before and after) are fitted to the temperatures measured by the thermocouple by adjusting the values of a_1 and a_2 . The result gives $1.52T = \Delta\phi + 1.35c + 0.079$, where the constant term is the contribution from the reference path.

Figure 2 shows a one-dimensional (1D) section of the 2D temperature field across the front obtained by interferometry together with the 1D temperature profile measured by the thermocouple. The result shows a good agreement between the two datasets along the entire profile despite the fact that only the temperatures far from the front have been used to scale the interferometric data. We point out that the correction of the phase field by the absorption image must be done in order to superpose the two datasets. The precision on the temperature measurement depends on the accuracy of the optical intensity recording on $\Delta\phi$ and Δc which is here $\sim 0.4\%$, and on the relative accuracy of the thermocouple, $\Delta T \pm 0.05$ °C. Under these conditions a precision of about 0.05 °C on the temperature is achieved by our method.

Eventually the calibration of T along one line is used to compute a full 2D image of the temperature field (Fig. 3), which can give informations on fingering of exothermic CT fronts for which only concentration field measurements were available up to now [17–19]. The first striking property of the temperature field is to be localized around the reaction front. As already shown by the thermocouple measurement on one point (Fig. 2) and confirmed on the full 2D picture (Fig. 3), heat losses through the walls are important as a decrease of the temperature is observed at the back of the front. The influence of such heat losses on the dynamics has already been studied in cooperative types of families where solutal and thermal contributions to the density jump across the front both have the same sign [20,23]. There, heat losses have been shown to drastically affect the stability diagram of cooperative fronts with regard to the insulated case [23] and to modify the structure of the flow field around the front [20]. No equivalent theoretical study is available up to now

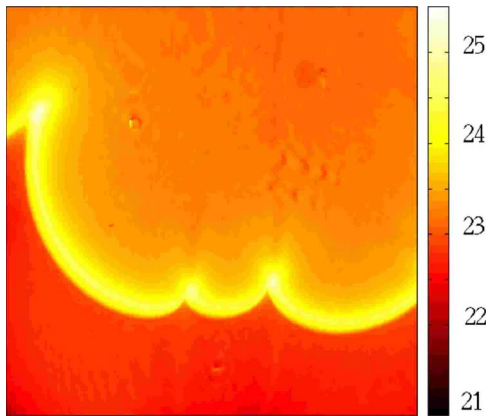


FIG. 3. (Color online) Reconstructed and calibrated 2D temperature field corresponding to the dynamics of Fig. 1.

for antagonist families. Measurements of 2D temperature fields as shown in Fig. 3 should provide precious information to validate future theoretical research in that area.

More strikingly, Fig. 3 shows the presence in the cusp of the fingers of hot spots where T reaches $25.5\text{ }^{\circ}\text{C}$, a value larger than the maximum temperature measured in the front by the thermocouple and larger than the adiabatic temperature [9]. This is important information that would have remained unnoticed here if one had only the single thermocouple signal of Fig. 2. The fact that the 2D temperature

spectrum is larger than the maximum T measured by the thermocouple shows, in particular, the efficiency of the quantitative reconstruction method able to catch the modulation of the temperature field transverse to the direction of propagation of the front. The hot spots observed result from the fact that cusps are the zone where fresh reactants are concentrated by convective rolls enhancing locally the reaction rate and hence the temperature. This is clear evidence that the coupling between exothermic reactions and diffusion and convective processes can lead to new dynamics, the study of which will benefit from the optical technique described here.

As a conclusion, we have developed an optical method to study spatiotemporal dynamics due to combined solutal and thermal effects in simple transparent reactors. This technique has allowed us to evidence the presence of hot spots in the fingering of exothermic autocatalytic CT fronts. It provides simultaneous measurements of full 2D concentration and temperature fields which is of importance to analyze buoyancy or Marangoni driven instabilities in both reactive and nonreactive homogeneous or two-layer systems.

Help from T. Tóth, D. Horváth, A. Tóth, and D. Lima in the use of the CT reaction is gratefully acknowledged. This work was supported by the project ARCHIMEDES of the Communauté française de Belgique (Grant No. ARC2004-09) and by Prodex of the European Space Agency.

-
- [1] A. Davaille, *Nature (London)* **402**, 756 (1999).
- [2] J. S. Turner, *Buoyancy Effects in Fluids* (Cambridge University Press, Cambridge, UK, 1973).
- [3] M. Schröter, K. Kassner, I. Rehberg, J. Claret, and F. Sagués, *Phys. Rev. E* **66**, 026307 (2002).
- [4] K. Eckert and A. Grahn, *Phys. Rev. Lett.* **82**, 4436 (1999).
- [5] D. Bratsun, Y. Shi, K. Eckert, and A. De Wit, *Europhys. Lett.* **69**, 746 (2005).
- [6] A. Zalts, C. El Hasi, D. Rubio, A. Urena, and A. D’Onofrio, *Phys. Rev. E* **77**, 015304(R) (2008).
- [7] J. A. Pojman, R. Craven, A. Khan, and W. West, *J. Phys. Chem.* **96**, 7466 (1992).
- [8] B. McCaughey, J. A. Pojman, C. Simmons, and V. A. Volpert, *Chaos* **8**, 520 (1998).
- [9] V. M. Ilyashenko and J. A. Pojman, *Chaos* **8**, 285 (1998).
- [10] M. Garbey, A. Taïk, and V. Volpert, *Q. Appl. Math.* **56**, 1 (1998).
- [11] J. A. Pojman and I. R. Epstein, *J. Phys. Chem.* **94**, 4966 (1990).
- [12] J. A. Pojman, I. R. Epstein, and I. Nagy, *J. Phys. Chem.* **95**, 1306 (1991).
- [13] I. Nagy and J. Pojman, *Chem. Phys. Lett.* **200**, 147 (1992).
- [14] I. Nagy, A. Keresztessy, and J. Pojman, *J. Phys. Chem.* **99**, 5385 (1995).
- [15] D. A. Vasquez, B. F. Edwards, and J. W. Wilder, *Phys. Fluids* **7**, 2513 (1995).
- [16] M. Böckmann, B. Hess, and S. C. Müller, *Phys. Rev. E* **53**, 5498 (1996).
- [17] T. Bánsági, Jr., D. Horváth, A. Tóth, J. Yang, S. Kalliadasis, and A. De Wit, *Phys. Rev. E* **68**, 055301(R) (2003).
- [18] T. Bánsági, Jr., D. Horváth, and A. Tóth, *Chem. Phys. Lett.* **384**, 153 (2004).
- [19] G. Casado, L. Tofaletti, D. Müller, and A. D’Onofrio, *J. Chem. Phys.* **126**, 114502 (2007).
- [20] L. Šebestíková, J. D’Heroncourt, M. J. B. Hauser, S. C. Müller, and A. De Wit, *Phys. Rev. E* **75**, 026309 (2007).
- [21] T. Tóth, D. Horváth, and A. Tóth, *Chem. Phys. Lett.* **442**, 289 (2007).
- [22] S. Kalliadasis, J. Yang, and A. De Wit, *Phys. Fluids* **16**, 1395 (2004).
- [23] J. D’Heroncourt, S. Kalliadasis, and A. De Wit, *J. Chem. Phys.* **123**, 234503 (2005).
- [24] J. D’Heroncourt, A. Zebib, and A. De Wit, *Phys. Rev. Lett.* **96**, 154501 (2006).
- [25] J. D’Heroncourt, A. Zebib, and A. De Wit, *Chaos* **17**, 013109 (2007).
- [26] M. Britton, *J. Phys. Chem. A* **110**, 5075 (2006).
- [27] V. Zhivonitko, I. Koptug, and R. Sagdeev, *J. Phys. Chem. A* **111**, 4122 (2007).
- [28] C. Shakher and A. K. Nirala, *Opt. Lasers Eng.* **31**, 455 (1999).
- [29] J. Mehta, *Appl. Opt.* **29**, 1924 (1990).
- [30] T. Kreis, *J. Opt. Soc. Am. A* **3**, 847 (1986).
- [31] M. Takeda, H. Ina, and S. Kobayashi, *J. Opt. Soc. Am.* **72**, 156 (1982).